Stability and plasmatic protein binding of novel zidovudine prodrugs: Targeting site ii of human serum albumin

Esteban M. Schenfeld, Sergio R. Ribone, Mario A. Quevedo

PII: S0928-0987(18)30031-9
DOI: https://doi.org/10.1016/j.ejps.2018.01.024
Reference: PHASCI 4374

To appear in: *European Journal of Pharmaceutical Sciences*

Received date: 21 November 2017
Revised date: 27 December 2017
Accepted date: 10 January 2018

Please cite this article as: Esteban M. Schenfeld, Sergio R. Ribone, Mario A. Quevedo , Stability and plasmatic protein binding of novel zidovudine prodrugs: Targeting site ii of human serum albumin. The address for the corresponding author was captured as affiliation for all authors. Please check if appropriate. Phasci(2017), https://doi.org/10.1016/j.ejps.2018.01.024

Stability and plasmatic protein binding of novel zidovudine prodrugs: targeting site ii of human serum albumin

Esteban M. Schenfeld,[a] Sergio R. Ribone[a] and Mario A. Quevedo[*a]

[a] *Unidad de Investigación y Desarrollo en Tecnología Farmacéutica (UNITEFA, CONICET), Departamento de Ciencias Farmacéuticas, Facultad de Ciencias Químicas, Universidad Nacional de Córdoba, Córdoba, X5000HUA, Argentina.* [*]*E-mail: alfredoq@fcq.unc.edu.ar; Tel: +54-351-53538*

ABSTRACT

Despite its vastly demonstrated clinical efficacy, zidovudine (AZT) exhibits several suboptimal pharmacokinetic properties. In particular, its short plasmatic half-life ($t_{1/2}$~1 h) is related to its low bound fraction to whole plasmatic proteins and in particular to human serum albumin (HSA). The design of prodrugs constitutes a promising strategy to enhance AZT pharmacokinetic properties, including its affinity for HSA. Recently, we reported the synthesis and chemical stability evaluation of three novel prodrugs of AZT obtained by derivatization with dicarboxylic acids (**1-3**). In this work, we present the design, synthesis and evaluation of chemical and enzymatic stabilities of a novel series of double prodrugs of AZT obtained by derivatization of **1-3** with a methylated *l*-phenylalanine moiety (**4-6**). In addition, the plasmatic protein binding properties were studied both by experimental and theoretical techniques. Prodrugs **4-6** were found to be relatively stable at pH 7.4 ($t_{1/2}$ between 4.1 and 57.8 h), while also demonstrated adequate stabilities in human plasma at 37 °C ($t_{1/2}$ between 1.0 and 2.1 h). Also, prodrugs **4-6** were able to regenerate AZT at a rate that depended on the length of the alkyl chain in **1-3**. Additionally, **4-6** exhibited a significantly increased binding to plasmatic proteins (between 52.1 and 72.5 %) with respect to AZT (12%) and **1-3** (between 26-34%). It is noteworthy that the displacement experiments with HSA site I and II markers, demonstrated that **4-6** bound to a different site than that of AZT and **1-3**. Molecular modeling studies (i.e. molecular docking and free energy of binding analysis) were applied to shed light at an atomistic level on the pharmacodynamic properties driving the interaction of **4-6** with HSA. Overall, the present work provides a state of the art contribution to the design and development of novel prodrugs of AZT with optimized pharmacokinetic properties.

Keywords: Zidovudine, prodrugs, Human Serum Albumin, Protein Binding, Molecular Modeling.

1. INTRODUCTION

Nucleoside reverse transcriptase inhibitors (NRTIs) were the first family of drugs approved by the Food and Drug Administration (FDA) to treat human immunodeficiency virus type-1 (HIV-1) infection,[1] the etiological agent causing the acquired immunodeficiency syndrome (AIDS) in humans. Among NRTIs, zidovudine (AZT, Figure 1.a) constitutes a key component of the highly active antiretroviral therapy (HAART) protocols currently used to treat AIDS.[1, 2] Despite its vastly demonstrated clinical efficacy, AZT exhibits several suboptimal pharmacokinetic properties, feature that often limits it efficacy and safety. Oral absorption of AZT is rapid and can be considered as complete; however first-pass metabolism significatively reduces its bioavailability. In particular, AZT is actively metabolized in liver by conjugation on it 5´OH position with glucuronic acid,[3] with glucurosyltransferase (isoform UGT2B7) being responsible of this catalysis.[4] Also cytochrome P450 is able to catalyze the reduction of the azido moiety present in AZT, originating the inactive compound 3'-amino-3'- deoxythymidine. The elimination half life of AZT is 1.1 hours,[5] with about 29% of the drug being eliminated unchanged in the urine and about 45% being excreted as the glucuronide. Upon absorption, AZT is bound in relatively low fractions to plasmatic proteins (30-38% in whole plasma and ~12% to pure human serum albumin (HAS)).[6] It also exhibits a short elimination half life of around 1.1 hours. In overall, the above presented pharmacokinetic properties results in the necessity of administering relatively high doses of drug in order to reach and maintain effective antiviral concentrations in plasma. This situation frequently leads to the occurrence of severe toxic effects and a low adherence of the patients to the antiretroviral treatment.[5, 7] In this context, numerous studies have dealt with strategies aimed at the optimization of the pharmacokinetic properties of AZT as a way of increasing its efficacy and safety, w.ith particular emphasis being focused in enhancing its plasmatic protein binding properties.

Figure 1

HSA is the main protein present in plasma, and is responsible for binding and transporting neutral and acidic compounds throughout the body.[8] Binding to plasmatic proteins constitutes a phenomena that determines the free drug concentration within body

fluids, both intra and extravascular, and as such constitutes a feature that needs to be carefully examined when attempting to optimize the efficacy and safety of a drug.[9] Structurally, HSA is formed by a single polypeptide chain bearing three domains, with each one containing two subdomains (Figure 2.a). To date, four main binding sites within the HSA molecule have been described, of which sites I and II (Figure 2.a,c) bind most of the drugs currently used in pharmacotherapy.[8] Characterizing the site within HSA to which drugs bind is of particular relevance, since drug-drug interactions may occur as a consequence of competition between co-administered drugs.[10, 11]

Figure 2

Significant efforts have been made to overcome AZT suboptimal pharmacokinetic properties by applying different chemical strategies. In particular, the design of prodrugs constitutes a very useful approach towards the possibility of improving most of the pharmacokinetic properties of AZT;[12-16] it is especially focused on the possibility of increasing its bound fraction to HSA and to modulate its cytotoxicity. AZT requires several phosphorylation steps on it 5´OH position in order to gain bioactivity, process that is selectively catalized by cytosolic thymidine kinase enzymes.[17] In this way, the chemical modification on the 5´OH position of AZT (i.e. activation by phosphorylation and inactivation by glucuronidation), determines a delicate balance related to its therapeutic efficacy and safety (Scheme 1). Since, only the unbound fraction to plasmatic proteins is available for enzymatic modification of the 5´OH, enhancing the affinity for HSA may represent profound changes both in the pharmacodynamic and pharmacokinetic properties of AZT.

Scheme 1

In this way many prodrugs have been prepared by derivatizing the 5´OH of AZT in order to obtain inactive compounds requiring a chemical and/or enzymatic hydrolytic step prior to exhibiting bioactivity.In line with these efforts, we have previously reported the obtention of prodrugs of AZT linking ester and amide moieties at the 5´OH position to obtain both “single” and “double” prodrugs.[14-16, 18-21] As an example, oxalic acid (AZT-Ox) was used as linker chain between AZT and different essential aminoacids (Fig

1.b). Although some of these prodrugs showed promising biological activities as measured in anti HIV *in vitro* assays,[19] they had a poor resistance to chemical and enzymatic hydrolysis, which was also accompanied by a limited bound fraction to HSA.[6, 22-25] Recently, we reported the synthesis and chemical stability evaluation of three novel prodrugs of AZT obtained by derivatization with different dicarboxylic acids (**1-3**, Figure 1.c): succinic (**1**), glutaric (**2**) and adipic (**3**) acids.[18] These single prodrugs exhibited adequate chemical stabilities at different pH values (2 - 7.4).[18]

In order to continue with the development of the above mentioned prodrugs, in the present work we report the design, synthesis and evaluation of the chemical and enzymatic stability of a novel series of AZT double prodrugs obtained by further derivatizing prodrugs **1-3** with a methylated *l*-phenylalanine moiety (**4-6**, Figure 1.d). In addition, their HSA binding properties were exhaustively studied by combining experimental and theoretical techniques in light of further evaluation of their biopharmaceutical behavior. The phenylalanine moiety was selected among natural aminoacids as a model endogenous scaffold since it has been reported to interact with carrier proteins in different tissues within the organism, including some of those that are considered as HIV-1 reservoirs.[26, 27] In addition, the methylation of the aminoacid was carried out to obtain lipophilic species at all physiological pH values and confer adequate bioavailability.

Overall, both experimental and theoretical methods were combined to obtain and study novel AZT prodrugs that exhibited adequate chemical and enzymatic stability profiles with a significantly increased protein bound fractions to human plasma proteins compared to the leader compound. Based on the presented results, it is possible to state that prodrugs **4-6** are very promising molecules that merit further development as part of preclinical studies in the search of efficient anti HIV agents.

2. EXPERIMENTAL SECTION

2.1. Chemicals and reagents

All chemical reagents were obtained from commercial sources (Sigma-Aldrich). AZT was generously provided by Filaxis Laboratories (Buenos Aires, Argentina). Acetonitrile (ACN), dichloromethane (DCM), chloroform, dimethyl sulfoxide (DMSO), acetone and

methanol were of analytical grade. Buffer solutions were prepared as follows: phosphate buffers (100 mM): (a) pH 2.0: 0.3 mL/mL H_3PO_4 (b) pH 7.4: (8.63 mg/mL Na_2HPO_4; 4.70 mg/mL NaH_2PO_4) and (C) pH 10.0: (8.63 mg/mL Na_2HPO_4), and PBS buffer pH 7.4 (NaCl 8.01 g/L, KCl 0.20 g/L, Na_2HPO_4 1.42 g/L,KH_2PO_4 0.27 g/L) all of which were prepared using milli-Q water. For quantification of samples by means of HPLC, milli-Q water and HPLC grade methanol and ACN were used for the mobile phase and sample preparation.

2.2. Synthetic protocols

Compounds **1-3** and the *l*-phenylalanine methyl ester were prepared as previously reported.[18] Prodrugs **4-6** were synthesized by reacting 1 eq. of **1-3**, 1.5 eq. of N´,N´-dicyclohexylcarbodiimide (DCC), 1.5 eq. of ethyl cyanoglyoxylate-2-oxime (Oxyma Pure ®) and 1 eq. of N,N-diisopropylethylamine (DIPEA) dissolved in 10 mL of anhydrous chloroform. The reaction mixture was maintained under magnetic stirring for 15 minutes (min) in an ice bath after which, 2 eq. of *l*-phenylalanine methyl ester (Phen-O-met) were added. The resulting suspension was kept at room temperature overnight and filtered and the resulting solution was extracted with a 2M HCl solution (3 x 10 mL). The organic phase was evaporated to dryness and the residue was redissolved in a buffer pH 2:acetone (80:20) mixture (20 mL). This solution was subjected to normal-phase flash chromatography using Silica gel 60 PF_{254} (Merck) and eluted with buffer pH2:acetone mixtures (80:20 x 50 mL; 70:30 x 50 mL; 60:40 x 100mL). The final solvent fraction was collected and the acetone was evaporated under vacuum. The resulting aqueous solution was extracted with DCM (3 x 10 mL). Then, the organic phase was dried over sodium sulfate, filtered and evaporated to dryness. The desired product was obtained as a white solid in good yields. The corresponding structures were confirmed by ^{1}H and ^{13}C NMR using a Bruker Avance II 400 spectrometer and acetone-d6 (99.9%, Sigma) as solvent. In addition, **4-6** were characterized by high resolution mass spectrometry (HRMS) using a Bruker Daltonics micro TOF QII LC-MS equipped with an electrospray ionization (ESI) interphase configured in positive mode.

3´-Azido-3´-deoxy-5´-O-succinyl-N-methoxyphenylalaninethymidine (4): This prodrug was obtained by condensing 3´-azido-3'-deoxy-5'-O-succinylthymidine acid (**1**) and *l*-phenylalanine methyl ester. The corresponding product was obtained in yields of

63%, mp: 144-145 °C. ^{13}CNMR (400 MHz, acetone-d6, TMS): d (ppm) = 10.8 (C11´´), 11.61 (C7), 14.98 (C12´´), 25.01 (C10´´), 29.60 (C 2´´), 29.80 (3´´), 36.51 (C 2´), 37.42 (C 8´´), 51.06 (C 5´), 56.15 (C 9´´), 60.54 (C 6´´), 62.99 (C 3´), 81.63 (C4´), 84.32 (C 1´), 110.36 (C 5), 135.69 (C 6), 150.33 (C 2), 163.27 (C 4), 170.98 (C 1´´), 171.920 (C 4´´), 172.20 (C 7´´). ^{1}H NMR (400 MHz, Acetone, TMS): d (ppm) = 0.75 (M, 6H, J = 7.5 Hz, 11´´-12 ´´-H), 1.72 (M, 3H, J = 1.2 Hz, 7-H), 1.92 (M, 2H, J = 2.01 Hz, 10´´-H), 2.31 (M, 1H, J = 12.3 Hz, 2b´-H), 2.42 (M, 1H, J= 13.9Hz, 2a´-H), 2.52 (M, 4H, J = 16.3 Hz, 2'' y 3´´-H), 3.54 (S, 3H, J = 18.4 Hz, 8´´-H), 3.94 (M, 1H, J = 3.88 Hz, 4´-H), 4.15 (DM, 1H, J = 3.6 Hz, 5b´-H), 4.31 (DM, 1H, J = 3.6 Hz, 5a´-H), 4.34 (M, 1H, J = 4.01 Hz, 9´´-H), 4.38 (DM, 1H, J = 5.46 Hz, 3´-H), 6.10(T, 1H, J = 24.4 Hz, 1´-H), 7.41 (D, 1H, J = 1.168 Hz, 6H). HRMS (ESI) m/z calculated for $C_{24}H_{28}N_6O_8$ Na $[M+nNa]^+$: 551.1861, found 551.1855.

3´-Azido-3´-deoxy-5´-O-glutaryl-N-methoxyphenylalaninethymidine (5): This prodrug was obtained by condensing 3´-azido-3´-deoxy-5´-O-glutarylthymidine acid (**2**) and *l*-phenylalanine methyl ester. The corresponding product was obtained in yields of 65%, mp: 150-151°C. ^{13}CNMR (400 MHz, acetone-d6, TMS): d (ppm) = 11.70 (C7), 20.62 (C3´´), 32.68 (C4´´), 34.18 (C2´) 36.16 (C2´´), 37.41 (C 10´´), 51.35 (C 9´´), 53.51 (C 7´´), 60.82 (C 3´), 63.21 (C5´), 81.49 (C4´), 84.64 (C 1´), 110.32 (C 5), 126.61 -128.28 (C 12´´-17´´), 129.17 (C 9´´), 135.74 (C 6), 150.32 (C 2), 163.31 (C 4), 171.49 (C 1´´), 172.04 (C 5´´), 172.42 (C 8´´). ^{1}H NMR (400 MHz, Acetone, TMS): d (ppm) = 1.70 (D, 3H, J = 1.2 Hz, 7-H), 2.11 (T, 2H, J = 14.7 Hz, 4´´-H), 2.24 (M, 1H, J = 17.16 Hz, 2´´H), 2.33 (M, 1H, J = 26.2 Hz, 3b´´-H), 2.41 (T, 1H, J =7.24 Hz, 2´-H), 2.44 (M, 1H, J = 27.8 Hz, 3a´´-H), 2.83 (C, 1H, J = 22.4 Hz, 10b´´-H), 2.99 (C, 1H, J = 19.4 Hz, 10a´´-H), 3.51 (S, 3H, J = 18.4 Hz, 9´´-H), 3.96 (C, 1H, J = 13.72 Hz, 4´-H), 4.17 (M, 1H, J = 15.88 Hz, 5b´-H), 4.27 (M, 1H, J= 16.8, Hz, 5a´-H), 4.39 (M, 1H, J= 18.6 Hz, 3´-H), 4.58 (M, 1H, J =22.2 Hz, 7´´-H), 6.11 (T, 1H,J =13.12 Hz, 1´-H), 7.12 (M, 5H, J = 31.7 Hz, 12´´-16´´-H), 7.36 (S, 1H, J = 1.16 Hz, 6-H). HRMS (ESI) m/z calculated for $C_{25}H_{30}N_6O_8$ Na $[M+nNa]^+$: 565.2017, found 565.2023.

3´-Azido-3´-deoxy-5´-O-adipyl-N-methoxyphenylalaninethymidine (6): This prodrug was obtained by condensing 3´-azido-3´-deoxy-5´-O- adipylthymidine acid (**3**) and *l*-phenylalanine methyl ester: The corresponding product was obtained in yields of 61%, mp:

159–160 °C. 13CNMR (400 MHz, acetone-d6, TMS): d (ppm) = 11.67 (C7), 24.12 (C3´´), 24.72 (C4´´),33.34 (C2´) 36.47 (C2´´-5´´), 37.44 (C 11´´), 51.29 (C 10´´), 53.49 (C 8´´), 60.85 (C 3´), 63.22 (C5´), 81.49 (C4´), 84.69 (C 1´), 110.25 (C 5), 126.57-129.18 (C 12´´-17´´), 135.74 (C 6), 150.29 (C 2), 163.27 (C 4), 171.76 (C 1´´), 172.02 (C 6´´), 172.42 (C 9´´). ^{1}H NMR (400 MHz, Acetone, TMS): d (ppm) = 1.44 (M, 4H, J = 36.8 Hz, 3´´-4´´-H), 1.71 (M, 3H, J = 13.6 Hz, 7-H), 2.25 (M, 2H, J = 24.4 Hz, 2´-H), 2.39 (M, 4H, J = 88.5 Hz, 2´´-5´´H), 2.83 (M, 1H, J =36.8 Hz, 11b´´-H), 2.99 (M, 1H, J =36.0 Hz, 11a´´-H), 3.52 (S, 3H, J = 18.4 Hz, 10´´-H), 3.96 (M, 1H, J = 33.6 Hz, 4´-H), 4.18 (DM, 1H, J = 30.4 Hz, 5b´-H), 4.26 (DM, 1H, J= 30.0, Hz, 5a´-H), 4.39 (M, 1H, J= 41.2 Hz, 3´-H), 4.58 (M, 1H, J =40.0 Hz, 8´´-H), 6.08 (T, 1H,J =36.0 Hz, 1´-H), 7.11 (M, 5H, J = 70.0 Hz, 13´´-17´´-H), 7.37 (S, 1H, J = 13.6 Hz, 6-H). HRMS (ESI) m/z calculated for $C_{26}H_{32}N_6O_8$ Na $[M+nNa]^+$: 579.2174 found 579.2161.

2.3. High performance liquid chromatography (HPLC) analyses

HPLC analyses were done using a Jasco chromatograph equipped with a quaternary pump and a Jasco Multiple Wavelength detector (Jasco UV- 2077 Plus) set at 270 nm. To perform chromatographic separations, a Phenomenex Synergy Fusion C18 analytical column (4.0 x 250 mm, 5 mm particle size) coupled to a Phenomenex Security Guard Fusion RP (4.0 x 30 mm) guard column was used. Chromatographic analyses were carried out using mobile phase gradients at a flow rate of 1 mL/min as follows: 0-2.5 mins: a mixture of a pH 2.0 phosphate buffer (0.1 mM): methanol (53:47, v/v), with a linear change between 2.5-9.5 mins to a 30:70 v/v composition. The mobile phase composition was kept constant from 9.5-12.0 mins. To ensure the re-equilibration of the mobile phase composition and the column conditions, the solvent gradient was reverted to initial conditions for 4.0 mins before the next injection was performed. The total run time for each injection was 15 min, with a sample injection volume of 10 μL.

2.4. Sample preparation procedures

Samples intended for HPLC analysis were prepared by means of a solid phase extraction (SPE) methodology using Strata-X Phenomenex SPE cartridges. The corresponding procedure involved five analytical steps: (a) cartridges were preconditioned by sequentially adding 2.0 mL of methanol followed by (b) an equilibration step with 2.0 mL of pH 2 (100

mM) phosphate buffer. Before loading the cartridge, 80 µL of a HCl 2M solution and 50 µL of the corresponding internal standard IS solution (compound **2** (0.15 mg/mL) for the analysis of **4** and **6** and compound **1** (0.15 mg/mL for the analysis **5**) were added to the sample, homogenized, and (c) applied to the preconditioned cartridge at a flow rate of 1 drop/s and dried under vacuum for 1 min. Afterwards, the (d) elution of the analytes was performed using 1mL of HPLC grade ACN, which was then (e) evaporated to dryness under a N_2 stream at 40 °C, and stored at -20 °C. On the day of analysis, the samples were redissolved in 200 µL of a phosphate a buffer pH 2: methanol (80:20) mixture and subjected to HPLC analysis as stated before.

2.5. Chemical and enzymatic stability studies

The chemical stability of **4-6** was studied at pH 2.0, 7.4 and 10.0 using the corresponding phosphate buffers. A stock solution (1.0 mg/mL) of each prodrug was prepared in DMSO, from which the corresponding working solutions (4.5×10^{-6} M) were prepared by adding 60 µL of the stock solution to 25 mL of buffer. Ten aliquots (2 mL) were withdrawn from the working solution, placed into sealed vials and incubated in a water bath at 37 °C. Samples intended for analysis were collected at convenient time intervals for each compound and assay condition.

For the enzymatic stability studies, stock solutions (10.0 mg/mL) of each prodrugs were prepared in DMSO. An aliquot (60 µL) of each stock solution was added to 2 mL of human plasma that was preincubated at 37 °C to attain the final working concentration (5.5×10^{-4} M). Aliquots of the spiked plasma (50 µL) were withdrawn at convenient time intervals and diluted with 2 mL of pH 2.0 phosphate buffer prior to being subjected to sample preparation and HPLC analysis. Fresh human plasma was generously supplied by the *Instituto de Hematología, Hemoterapia y Banco de Sangre, Universidad Nacional de Córdoba, Argentina*.

2.6. Plasmatic protein binding assays

Fresh human plasma was filtered over glass wool before use and the concentration of total proteins (TP) and HSA were determined using commercially available kits (*Proti 2*, Weiner lab®, Argentina, and *Albúmina*, Weiner lab®, Argentina, for TP and HSA, respectively) according to the instructions provided by the manufacturer. All samples used

in the binding assays exhibited TP concentrations between 5.5–5.8 g/dL and HSA concentrations between 3.6–4.1 g/dL.

To perform the binding assays, stock solutions (1 mg/mL) of **4**-**6** were diluted in pH 7.4 PBS buffer to a concentration of 0.01 mg/mL. Aliquots (600 µL) of the resulting working solutions were incubated with 600 µL of human plasma at 37 °C under gentle stirring for 10 min. The corresponding protein bound fraction was separated from the free fraction by ultrafiltration using a micropartition system (Centrifree®UF, Millipore, 1 mL) equipped with an Ultracel YM-T membrane (cut-off 30 KDa). Ultrafiltration devices were centrifuged at 2000 rpm for 5 min, collecting less than 25% of the initial volume in the ultrafiltrate in order to avoid displacements in the binding equilibrium between the drug and the corresponding protein.[6] The samples intended for analysis were prepared by mixing 100 µL of ultrafiltrate and 50 µL of the corresponding internal standard IS (AZT-Glu (**2**) 0,015 mg/mL for **4** and **6**; AZT-Suc (**1**) 0,015 mg/mL for **5**). Binding assays were performed in quintuplicate.

Three experimental conditions were assayed: a) pure human plasma only, b) human plasma spiked with salicylic acid (SAL), and c) human plasma spiked with diazepam (DZP).

The results are expressed as percentage of bound fraction (F_b) and were calculated using eq. [1]:

$$F_b = 100 - ((C_S/C_I) * 100) \qquad \textbf{eq. [1]}$$

where C_S corresponds to concentration quantified in the ultrafiltrate and C_I to the analyte concentration in the incubated plasma.

2.7. Molecular modeling studies

The initial structures of the simulated ligands were constructed using MarvinSketch v.16.2.15 developed by ChemAxon Ltd.[28] With respect to the structure of HSA, three different crystallographic structures were used as receptor templates: a) HSA in complex with AZT and Myr (PDB code: 3B9L),[29] b) the crystallographic complex between SAL, Myr and HSA (PDB code: 2I30)[30] and c) the complex between DZP, Myr, and HSA, which was constructed by combining PDB code: 2BXF [8] and PDB code: 1E7G.[31]

The complexes between the studied molecules and HSA were obtained by molecular docking simulations, which were performed using software packages developed by OpenEye Scientific Software.[32] The corresponding procedures consisted of three stages: a) ligand conformer library generation, which was performed by applying an energy threshold of 10 kcal/mol and using the OMEGA software,[33, 34] b) docking assays which were conducted by applying a fast rigid exhaustive docking approach as implemented in the FRED3 software [35, 36] and using the ChemGauss3 scoring function to evaluate and score the resulting docked poses. The final stage involved the c) docked pose extraction and visualization, which was performed using the VIDA v.4.3.0 software developed by OpenEye Scientific Software.[37] The lowest energy docked pose was selected for further analysis by means of free-energy of binding analysis.

Based on the complexes with HSA predicted by molecular docking, the free energy of binding was calculated using the MMPBSA.py [38] as implemented in AMBER16.[39] The *ff14SB* and GAFF [40] force fields implemented in AMBER16 were used to parameterize HSA and the corresponding ligands, respectively. The energy of binding was estimated by taking into account the solvation energies of the interacting molecules, in addition to the molecular mechanics (MM) energies. The contribution of polar solvation energies was computed using the generalized Born (GB) implicit solvent model, while the non-polar contribution to the solvation energy was calculated based on the solvent accessible surface area (SASA).[41]. Intermolecular interactions were computed and depicted using the VMD v.1.9.3. and LigPlot+ v.1.4.5 software.[42, 43]

3. RESULTS AND DISCUSSION

3.1. Synthesis of prodrugs 4-6

In a first step, prodrugs **1-3** were obtained following our previously reported procedure,[18] after which the synthesis of prodrugs **4-6** was conducted by condensing **1-3** and a phenylalanine methyl ester aminoacid (Scheme 2). The procedure implemented was straightforward and resulted in the obtention of the desired compounds with acceptable yields. Although several synthetic procedures have been used for this kind of condensation procedures,[44, 45] the OxymaPure/DCC coupling strategy, widely used for the synthesis of peptides, resulted in a simple and efficient procedure.[46-48] Also, the method

developed is expected to be feasible for being scaled up under safer conditions compared to the use of explosive benzotriazole derivatives.[46] It is noteworthy that the developed methodology allows the exploration of a wider chemical space for the diacid linker chain compared to classic methodologies in which cyclic anhydrides are used.[49] The possibility to explore a wide chemical space for the linker chain constitutes a key feature for the design of this kind of prodrugs, since (as will be presented later in this work), the biopharmaceutical properties of the resulting compound is highly dependent on the linker chain structure.

Scheme 2

3.2. Chemical and plasmatic stability

In order to assess the chemical and enzymatic stability of **4-6,** as well as their ability to regenerate the lead drug AZT, both the rate of chemical (pH 2-10) and enzymatic (human plasma) hydrolysis were determined (Table 1). We observed that all the compounds exhibited a pseudo-first order hydrolysis kinetics, with the corresponding concentration *vs.* time profiles being determined (Fig. S1-S3, Suppl. Mat.). All compounds showed to be stable at pH 2 for 24 hs. In relation to pH 7.4 and 10, the hydrolysis constant (*k*) and half life time ($t_{1/2}$) were calculated from the corresponding profiles and are shown in Table 1**.**

Table 1

From the chemical stability of the double prodrugs **4**-**6**, we observed that unlike the single prodrugs (**1**-**3**), the former were able to regenerate AZT at pH 7.4. The calculated $t_{1/2}$ values were 4.1, 7.5, and 57.8 hs for **4**, **5**, and **6**, respectively (Table 1). It is evident that the addition of the aminoacid scaffold to the single prodrug enhanced the reconversion of **4-6** to AZT, with the rate of this reconversion being strongly dependent on the length of the chain included in **1-3**. Under strongly alkaline conditions (pH 10), all the prodrugs exhibited a significantly higher hydrolysis rate, with all of them exhibiting $t_{1/2}$ values of 10 min or lower (Table 1). It is noteworthy that the unique chemical hydrolysis product originated from **4-6** corresponded to AZT, with no **1-3** being detected. This observation is consistent with the fact that amide moieties are more stable than esters.

From assays in whole plasma, it was found that the single prodrugs **1-3** displayed a high resistance to enzymatic cleavage (Table 1), regenerating only very small amounts of AZT

throughout the 24 h sampling interval. Compounds **4-6**, in contrast, were hydrolyzed at a rate strongly dependent on the structure of the compound and much faster than the single prodrugs **1-3**. Figure S3.a-c presents the corresponding concentration vs. the time profiles determined for prodrugs **4**-**6**, in which all the relevant species were quantified, i.e., AZT, the demethylated prodrug and the intact prodrug. As can be seen, in all cases the demethylated prodrug was generated by enzymatic hydrolysis, observing a rapid increase in its concentration and a second phase in which it was completely hydrolyzed. As expected, in all cases, the resulting final product was AZT. The enzymatic stability followed a similar trend to that of the chemical stability, with $t_{1/2}$ values of 1.0, 1.5 and 2.1 hs for **4**, **5**, and **6** respectively (Table 1, Fig. 3). In agreement with the chemical hydrolysis studies, the single prodrugs **1-3** were not detected during the assay, indicating that the plasmatic enzymes were not able to efficiently hydrolyzed the amide bond present in **4**-**6**.

Figure 3

3.3. Binding of 1-6 to plasmatic proteins: experimental studies

The bound fractions to whole plasma proteins was determined for **1-6** and compared to that of AZT (Table 2). Taking into account that HSA is the main plasmatic protein, two well-known HSA binding site displacers were used in order to identify the binding site for each prodrug: salicylic acid (SAL, site I marker) and diazepam (DZP, site II marker).[6, 50, 51]

In agreement with our previous studies,[6, 23] AZT exhibited a low bound fraction to plasmatic proteins (13.8±1.4 %). Conversely, the single prodrugs **1-3** displayed a moderate increase in their bound fractions (33.2, 26.8 and 34.1 for **1**, **2**, and **3**, respectively). Note that **1-3** exhibited a considerably higher bound fraction compared to AZT-Ox (10.4±1.8%),[6] as determined in a previous report. Clearly, the increase in the chain length of **1-3** separating the AZT scaffold and the ionized carboxylate moiety allowed a more efficient binding mode to HSA. From the displacement assays, we observed that SAL (site I marker) was able to efficiently displace the bound fractions of **1-3** (8.1, 1.8, and 4.8 % for **1**, **2**, and **3**, respectively), evidencing the fact that they were bound to site I of HSA. These results are in agreement with the binding of AZT-Ox, as was previously reported.[6]

When the double prodrugs **4-6** were studied, considerably higher bound fractions with respect to AZT were found (52.1, 59.7 and 72.5 % for **4**, **5**, and **6**, respectively). From the displacement studies with SAL, we observed no reduction in the bound fractions, indicating that **4-6** were not bound to site I in HSA. In contrast, when the displacement was studied using DZP (site II marker), a reduction in the bound fraction was quantified, indicating that **4-6** were bound with a high affinity to site II. Consequently, we obtained both a higher affinity for HSA and a change in the site of binding by designing these double prodrugs.

Table 2

3.4. Binding of 1-6 to plasmatic proteins: theoretical studies

To study the mode of binding of **1-6** to HSA at an atomistic level, molecular modeling techniques (i.e. molecular docking and free-energy of interaction analysis) were performed. To accomplish these studies, the crystallographic structure of HSA complexed with AZT and Myr (PDB code: 3B9L) was used as structural template,[29] while the complex HSA with salicylic acid and Myr (PDB code: 2I30) was used to model displacement assays.[30]

Compounds **1-3** were docked to site I of HSA, observing that in all cases the lowest energy bound mode was characterized by the establishment of intermolecular interactions with the residues Tyr150, Ser192, Lys195, Gln196, Lys199, Val241, Cys245, Arg257, Ser287, His288 and Ala291 (Fig 4.a-c, Fig. S15). This binding mode is homologous to that observed for AZT in X-ray studies.[29] Also, from the per-residue free energy of interaction analysis (Table 3) it can be observed that **1-3** established strong electrostatic interactions with Arg257 (-8.62, -13.23 and -14.04 Kcal/mol, respectively), leading to an enhanced affinity for HSA compared to AZT, which is not able to establish stabilizing interactions with this residue (1.15 Kcal/mol). The electrostatic interactions with Arg257 is crucial to the binding of acidic drugs to HSA, such as SAL (-13.45 Kcal/mol), which is also consistent with the displacement of **1-3** elicited by this site I marker. In addition, prodrugs **1** and **2** were able to establish interactions with His288 (-5.66 and -1.49 Kcal/mol, respectively), which was not observed for SAL. The interaction with His288 is possible because the negatively charged carboxylic acid is oriented towards the vicinity of His288 by the linker chain spacer of two and three carbon atoms present in **1** and **2**, respectively. It

is noteworthy that the ΔG_{sum} values presented in Table 3 are in agreement with the bound fractions determined experimentally (Table 2), with higher interaction energies calculated for **1** and **3** compared to **2**. Also, the overall interaction energies calculated for **1**, **2** and **3** (-20.75, -18.10 and -20.28 Kcal/mol, respectively) are significantly higher than those calculated for AZT (-2.72 Kcal/mol). This observation is consistent with their enhanced affinity for plasmatic proteins observed experimentally.

Figure 4

Table 3

The binding of prodrugs **4-6** was modeled to HSA site II based on the results obtained in the displacement assays. To construct the receptor template, the structure corresponding to the crystallographic complex between HSA and DZP (PDB code: 2BXF)[8] was superimposed on the crystal structure of HSA with Myr (PDB code: 1E7G), after which the site II marker was pasted on the latter to generate the working receptor.

The binding to site II was modeled using DZP as reference (Fig. 5.a). When prodrugs **4-6** were docked in site II, it was found that the phenylalanine moiety was deeply buried within the site cavity (Figs. 5b-d, Fig. S16), while the AZT scaffold was oriented towards either the polar patch near the cavity entrance (Arg410, Tyr411 and Ser489) or towards the solvent exposed region lying outside the binding cavity (prodrug **6**). Table 4 presents the per-residue MMGBSA binding free energy analysis for the binding of DZP and **4-6** to site II. As can be seen DZP shares several interaction spots with **4-6** (Glu383, Pro384, Leu387, Ile388, Asn391, Phe403, Leu407, Leu430, Gly434, Ala449, Glu450 and Leu453), which is consistent with the displacements observed experimentally. As can be observed, the binding of **4-6** is mostly stabilized by hydrophobic contacts, with extensive interactions being established with Ser342, Glu382, Pro486, Phe488, Ala490 and Leu491 (Table 4). It is evident that these relatively bulky and hydrophobic prodrugs are able to occupy an extensive buried area within site II. Also, the sum of interaction energies (ΔG_{sum}) calculated for **4-6** (-13.22, -14.13 and -19.26 Kcal/mol, respectively) are in agreement with the bound fractions observed experimentally, with the higher interaction energies and bound fractions being observed for prodrug **6** (72.8%). It is noteworthy that higher interaction energies were calculated for **4-6** compared to DZP, which is consistent with the limited capacity of the latter to displace the prodrugs bound to site II (Table 2).

Figure 5

Table 4

As mentioned above the chemical modification of prodrugs **4-6** produced a change in the HSA binding site selectivity with respect to AZT and prodrugs **1-3**. To further study the molecular basis behind this behavior, the binding of **4-6** to site I was simulated and the corresponding interaction energies were calculated (Table 5). As can be seen, unfavorable binding interactions with residues lying within site I were found (ΔG_{sum}: 3.88, 3.43, and 2.51 Kcal/mol for **4**, **5**, and **6**, respectively). In this case, the positively charged residues His288 and Arg257 did not establish stabilizing interactions, which is in agreement with the experimental findings that showed no affinity of **4-6** for this site. Thus, the presented methodology may also be useful to predict the binding site of this family of prodrugs to HSA.

Table 5

4. CONCLUSIONS

In this work, novel double prodrugs of AZT (**4-6**) were obtained by derivatization of single AZT prodrugs **1-3** with a methylated phenylalanine moiety. The reported synthetic protocol and associated purification procedures are simple and efficient, and as such are feasible to scale up the production of these kinds of prodrugs, if necessary. Also, key biopharmaceutical properties were profiled in view of further evaluating the performance and benefits of **4-6**, including their chemical and enzymatic stability and their corresponding plasma protein binding capabilities compared with the lead drug AZT. We found that the design and synthesis of prodrugs **4-6** resulted in compounds with improved biopharmaceutical properties (i.e. chemical and enzymatic stability and binding to plasmatic proteins) compared to the lead molecule AZT. Noteworthy, all of studied prodrugs were able to regenerate the lead molecule at an efficient rate under physiological conditions (pH 7.4 and human plasma). This observation represents a significant improvement in comparison with the single prodrugs **1-3**, which exhibited a high stability under the above mentioned conditions and were unable to regenerate AZT at therapeutic compatible rates.

Regarding the plasmatic protein binding, all the prodrugs (i.e. single and double) showed increased bound fractions compared with AZT, with **4-6** exhibiting the highest bound fractions. Remarkably, the single prodrugs **1-3** were bound to site I of HSA, while the double prodrugs **4-6** were bound to site II. Molecular modeling techniques were able to exhaustively describe at an atomic resolution the structural basis behind this behavior. Overall, the described protein binding properties represent potential, significant benefits for the novel developed prodrugs (**4-6**), since upon bioactivation and AZT regeneration in body fluids, no competition is expected for HSA binding, which leads to an improved biopharmaceutical profile of the parent drug. In addition to the enhanced biopharmaceutical properties, prodrugs **4-6** are expected to exhibit lower side effect than the lead compound AZT, since phosphorylation on the 5´OH position is blocked for the prodrugs.

The development of this family of prodrugs containing succinic, glutaric and adipic acid linked to a methylated phenylalanine moiety on the 5´OH position of AZT, resulted in a marked enhancement in their chemical and enzymatic stability properties and plasmatic protein binding capabilities compared to the prodrugs containing an oxalic acid linker that were reported previously by our group.[6, 23, 52]

In conclusion, the present work is a valuable effort to design and development of novel double prodrugs of AZT with optimized pharmacokinetic properties. Also, the potential of applying molecular modeling techniques to screen prospective plasmatic protein binding properties has been demonstrated. In particular, it has been shown that it is possible to further study a large set of modified essential aminoacids as scaffolds for the design and obtention of new prodrugs. Based on the reported findings, in a future work will be continued to evaluate additional aminoacids as chemical moieties for the design of safe and more efficient AZT prodrugs.

ACKNOWLEDGEMENTS

The authors gratefully acknowledge financial support from the Secretaria de Ciencia y Técnica of the Universidad Nacional de Córdoba (SECYT-UNC), the Consejo Nacional de Investigaciones Científicas y Técnicas (CONICET), and the Agencia Nacional de Promoción Científica y Técnica (ANPCyT). The authors would also like to thank the GPGPU Computing Group from the Facultad de Matemática, Astronomía y Física

(FAMAF), Universidad Nacional de Córdoba, Argentina, for providing access to computing resources. Mario A. Quevedo wishes to thank OpenEye Scientific Software and their Free Academic Licensing program for providing him with licenses to use the corresponding software packages.

REFERENCES

[1] E. De Clercq, G. Li, Approved antiviral drugs over the past 50 years, Clin. Microbiol. Rev., 29 (2016) 695-747.
[2] E. De Clercq, Antiretroviral drugs, Curr. Opin. Pharmacol., 10 (2010) 507-515.
[3] K.H.P. Moore, R.H. Raasch, K.L.R. Brouwer, K. Opheim, S.H. Cheeseman, E. Eyster, S.M. Lemon, C.M. Van der Horst, Pharmacokinetics and bioavailability of zidovudine and its glucuronidated metabolite in patients with human immunodeficiency virus infection and hepatic disease (AIDS clinical trials group protocol 062), Antimicrob. Agents Chemother., 39 (1995) 2732-2737.
[4] M.H. Court, S. Krishnaswamy, Q. Hao, S.X. Duan, C.J. Patten, L.L. Von Moltke, D.J. Greenblatt, Evaluation of 3′-azido-3′-deoxythymidine, morphine, and codeine as probe substrates for udp-glucuronosyltransferase 2B7 (UGT2B7) in human liver microsomes: Specificity and influence of the UGT2B7*2 polymorphism, Drug Metab. Dispos., 31 (2003) 1125-1133.
[5] E.R. Scruggs, A.J.D. Naylor, Mechanisms of zidovudine-induced mitochondrial toxicity and myopathy, Pharmacology, 82 (2008) 83-88.
[6] M.A. Quevedo, S.R. Ribone, G.N. Moroni, M.C. Briñón, Binding to human serum albumin of zidovudine (AZT) and novel AZT derivatives. Experimental and theoretical analyses, Bioorg. Med. Chem., 16 (2008) 2779-2790.
[7] G. D'Andrea, F. Brisdelli, A. Bozzi, AZT: An old drug with new perspectives, Curr. Clin. Pharmacol., 3 (2008) 20-37.
[8] J. Ghuman, P.A. Zunszain, I. Petitpas, A.A. Bhattacharya, M. Otagiri, S. Curry, Structural basis of the drug-binding specificity of human serum albumin, J. Mol. Biol., 353 (2005) 38-52.
[9] D.A. Smith, L. Di, E.H. Kerns, The effect of plasma protein binding on in vivo efficacy: Misconceptions in drug discovery, Nat. Rev. Drug Discov., 9 (2010) 929-939.
[10] L.-L. He, Z.-X. Wang, Y.-X. Wang, X.-P. Liu, Y.-J. Yang, Y.-P. Gao, X. Wang, B. Liu, Studies on the interaction between promethazine and human serum albumin in the presence of flavonoids by spectroscopic and molecular modeling techniques, Colloids Surf B Biointerfaces, 145 (2016) 820-829.
[11] F. Shiri, S. Shahraki, A. Shahriyar, M.H. Majd, Exploring isoxsuprine hydrochloride binding with human serum albumin in the presence of folic acid and ascorbic acid using multispectroscopic and molecular modeling methods, J. Photochem. Photobiol. B, 170 (2017) 152-163.
[12] P.N. Solyev, A.V. Shipitsin, I.L. Karpenko, D.N. Nosik, L.B. Kalnina, S.N. Kochetkov, M.K. Kukhanova, M.V. Jasko, Synthesis and Anti-HIV Properties of New Carbamate Prodrugs of AZT, Chem. Biol. Drug Des., 80 (2012) 947-952.

[13] G. Giacalone, H. Hillaireau, E. Fattal, Improving bioavailability and biodistribution of anti-HIV chemotherapy, Eur. J. Pharm. Sci., 75 (2015) 40-53.
[14] A. Dalpiaz, G. Paganetto, B. Pavan, M. Fogagnolo, A. Medici, S. Beggiato, D. Perrone, Zidovudine and ursodeoxycholic acid conjugation: Design of a new prodrug potentially able to bypass the active efflux transport systems of the central nervous system, Mol. Pharm., 9 (2012) 957-968.
[15] Y. Zhang, Y. Gao, X. Wen, H. Ma, Current prodrug strategies for improving oral absorption of nucleoside analogues, Asian Journal of Pharmaceutical Sciences, 9 (2014) 65-74.
[16] W. Li, Y. Chang, P. Zhan, N. Zhang, X. Liu, C. Pannecouque, E. De Clercq, Synthesis, in vitro and in vivo release kinetics, and anti-HIV activity of A sustained-release prodrug (mPEG-AZT) of 3′-azido-3′-deoxythymidine (AZT, Zidovudine), ChemMedChem, 5 (2010) 1893-1898.
[17] P.A. Furman, J.A. Fyfe, M.H. St Clair, K. Weinhold, J.L. Rideout, G.A. Freeman, S.N. Lehrman, D.P. Bolognesi, S. Broder, H. Mitsuya, Phosphorylation of 3'-azido-3'-deoxythymidine and selective interaction of the 5'-triphosphate with human immunodeficiency virus reverse transcriptase, Proc. Natl. Acad. Sci. U. S. A., 83 (1986) 8333-8337.
[18] S.R. Ribone, E.M. Schenfeld, M. Madrid, A.B. Pierini, M.A. Quevedo, Evaluation and synthesis of AZT prodrugs with optimized chemical stabilities: Experimental and theoretical analyses, New J. Chem., 40 (2016) 2383-2392.
[19] G.N. Moroni, P.M. Bogdanov, M.C. Briñón, Synthesis and in vitro antibacterial activity of novel 5′-O-analog derivatives of zidovudine as potential prodrugs, Nucleosides Nucleotides Nucleic Acids, 21 (2002) 231-241.
[20] M.A. Raviolo, J.S. Trinchero-Hernández, G. Turk, M.C. Briñón, Synthesis and antiretroviral evaluation of derivatives of zidovudine, J. Braz. Chem. Soc., 20 (2009) 1870-1877.
[21] S. Wannachaiyasit, P. Chanvorachote, U. Nimmannit, A novel anti-HIV dextrin–zidovudine conjugate improving the pharmacokinetics of zidovudine in rats, AAPS PharmSciTech, 9 (2008) 840.
[22] M.A. Quevedo, M.C. Briñón, In vitro and in vivo pharmacokinetic characterization of two novel prodrugs of zidovudine, Antiviral Res., 83 (2009) 103-111.
[23] M.A. Quevedo, G.N. Moroni, M.C. Briñón, Human serum albumin binding of novel antiretroviral nucleoside derivatives of AZT, Biochem. Biophys. Res. Commun., 288 (2001) 954-960.
[24] M.A. Quevedo, L.E. Nieto, M.C. Briñón, P-glycoprotein limits the absorption of the anti-HIV drug zidovudine through rat intestinal segments, Eur. J. Pharm. Sci., 43 (2011) 151-159.
[25] G.N. Moroni, M.A. Quevedo, S. Ravetti, M.C. Briñón, Lipophilic character of novel amino acid derivatives of zidovudine with anti HIV activity, J. of Liq. Chrom. & Rel. Tech., 25 (2002) 1345-1365.
[26] O. Yanagida, Y. Kanai, A. Chairoungdua, D.K. Kim, H. Segawa, T. Nii, S.H. Cha, H. Matsuo, J.-i. Fukushima, Y. Fukasawa, Human L-type amino acid transporter 1 (LAT1): characterization of function and expression in tumor cell lines, Biochimica et Biophysica Acta (BBA)-Biomembranes, 1514 (2001) 291-302.
[27] F.M. Sutera, V. De Caro, L.I. Giannola, Small endogenous molecules as moiety to improve targeting of CNS drugs, Expert Opin Drug Deliv, 14 (2017) 93-107.

[28] MarvinSketch, MarvinSketch v.16.2.15, in, ChemAxon Ltd.
[29] L. Zhu, F. Yang, L. Chen, E.J. Meehan, M. Huang, A new drug binding subsite on human serum albumin and drug–drug interaction studied by X-ray crystallography, J. Struct. Biol., 162 (2008) 40-49.
[30] F. Yang, C. Bian, L. Zhu, G. Zhao, Z. Huang, M. Huang, Effect of human serum albumin on drug metabolism: structural evidence of esterase activity of human serum albumin, J. Struct. Biol., 157 (2007) 348-355.
[31] A.A. Bhattacharya, T. Grüne, S. Curry, Crystallographic analysis reveals common modes of binding of medium and long-chain fatty acids to human serum albumin, J. Mol. Biol., 303 (2000) 721-732.
[32] OpenEye.Scientific.Software, in, OpenEye Scientific Software.
[33] Omega.2.4.3, in, OpenEye Scientific Software, Santa Fe, NM http://www.eyesopen.com.
[34] P.C.D. Hawkins, A.G. Skillman, G.L. Warren, B.A. Ellingson, M.T. Stahl, Conformer generation with OMEGA: Algorithm and validation using high quality structures from the protein databank and cambridge structural database, J. Chem. Inf. Model., 50 (2010) 572-584.
[35] M. McGann, FRED pose prediction and virtual screening accuracy, J. Chem. Inf. Model., 51 (2011) 578-596.
[36] S.F. Fred.3.0.0 OpenEye Scientific Software, NM http://www.eyesopen.com, in.
[37] VIDA.4.3.0, in, OpenEye Scientific Software, Santa Fe, NM http://www.eyesopen.com.
[38] B.R. Miller, T.D. McGee, J.M. Swails, N. Homeyer, H. Gohlke, A.E. Roitberg, MMPBSA.py: An efficient program for end-state free energy calculations, J. Chem. Theor. Comput., 8 (2012) 3314-3321.
[39] D.A. Case, D.S. Cerutti, T.E. Cheatham Iii, T.A. Darden, R.E. Duke, T.J. Giese, H. Gohlke, A.W. Goetz, D. Greene, N. Homeyer, S. Izadi, A. Kovalenko, T.S. Lee, S. LeGrand, P. Li, C. Lin, J. Liu, T. Luchko, R. Luo, D. Mermelstein, K.M. Merz, G. Monard, H. Nguyen, I. Omelyan, A. Onufriev, F. Pan, R. Qi, D.R. Roe, A. Roitberg, C. Sagui, C.L. Simmerling, W.M. Botello-Smith, J. Swails, R.C. Walker, J. Wang, R.M. Wolf, X. Wu, L. Xiao, D.M. York, P.A. Kollman, AMBER 2017, in, University of California, San Francisco, 2017.
[40] J. Wang, R.M. Wolf, J.W. Caldwell, P.A. Kollman, D.A. Case, Development and testing of a general amber force field, J. Comput. Chem., 25 (2004) 1157-1174.
[41] P.A. Kollman, I. Massova, C. Reyes, B. Kuhn, S. Huo, L. Chong, M. Lee, T. Lee, Y. Duan, W. Wang, O. Donini, P. Cieplak, J. Srinivasan, D.A. Case, T.E. Cheatham Iii, Calculating structures and free energies of complex molecules: Combining molecular mechanics and continuum models, Acc. Chem. Res., 33 (2000) 889-897.
[42] W. Humphrey, A. Dalke, K. Schulten, VMD: Visual molecular dynamics, J. Mol. Graph., 14 (1996) 33-38.
[43] A.C. Wallace, R.A. Laskowski, J.M. Thornton, LIGPLOT: A program to generate schematic diagrams of protein-ligand interactions, Protein Eng., 8 (1995) 127-134.
[44] P. KVSRG, K. Bharathi, B. Haseena Banu, Applications of peptide coupling reagents–An update, International Journal of Pharmaceutical Sciences Review and Research, 8 (2011) 108-119.
[45] C.A.G.N. Montalbetti, V. Falque, Amide bond formation and peptide coupling, Tetrahedron, 61 (2005) 10827-10852.

[46] R. Subirós-Funosas, R. Prohens, R. Barbas, A. El-Faham, F. Albericio, Oxyma: An efficient additive for peptide synthesis to replace the benzotriazole-based HOBt and HOAt with a lower risk of explosion, Chem. Eur. J., 15 (2009) 9394-9403.
[47] A. El-Faham, Z. Al Marhoon, A. Abdel-Megeed, F. Albericio, OxymaPure/DIC: An efficient reagent for the synthesis of a novel series of 4-[2-(2-acetylaminophenyl)-2-oxo-acetylamino] benzoyl amino acid ester derivatives, Molecules, 18 (2013) 14747-14759.
[48] A. El-Faham, Z. Al Marhoon, A. Abdel-Megeed, S.N. Khattab, A.A. Bekhit, F. Albericio, α-Ketoamino acid ester derivatives as promising MAO inhibitors, Bioorg. Med. Chem. Lett., 25 (2015) 70-74.
[49] P. Vlieghe, F. Bihel, T. Clerc, C. Pannecouque, M. Witvrouw, E. De Clercq, J.P. Salles, J.C. Chermann, J.L. Kraus, New 3′-azido-3′-deoxythymidin-5′-yl O-(ω-hydroxyalkyl) carbonate prodrugs: Synthesis and anti-HIV evaluation, J. Med. Chem., 44 (2001) 777-786.
[50] A. Divsalar, S. Khodabakhshian, Probing the binding site of a new synthesized anti-cancer compound to HSA via competitive ligand binding method, J. Mol. Liq., 206 (2015) 82-88.
[51] M.Z. Kabir, S.R. Feroz, A.K. Mukarram, Z. Alias, S.B. Mohamad, S. Tayyab, Interaction of a tyrosine kinase inhibitor, vandetanib with human serum albumin as studied by fluorescence quenching and molecular docking, J. Biomol. Struct. Dyn., 34 (2016) 1693-1704.
[52] M.A. Quevedo, S.A. Teijeiro, M.C. Briñón, Quantitative plasma determination of a novel antiretroviral derivative of zidovudine by solid-phase extraction and high-performance liquid chromatography, Anal Bioanal Chem, 385 (2006) 377-384.

Table 1. Chemical stability (pH 7.4 and 10.0) and plasmatic stability parameters for prodrugs **1-6** at 37°C.

Prodrug	Chemical Stability				Enzymatic Stability	
	pH 7.4		pH 10			
	k (min^{-1})	$t_{1/2}$ (min)	k (min^{-1})	$t_{1/2}$ (min)	k (min^{-1})	$t_{1/2}$ (min)
1	Stable*	Stable*	0.001±0.001*	630.1±2.1*	0.0001 ± 0.0001	8022.5±555.8
2	Stable*	Stable*	0.001±0.002*	462.1±5.3*	0.0005 ± 0.0001	1501.8±199.9
3	Stable*	Stable*	0.002±0.001*	385.1±2.6*	0.0003 ± 0.0001	2695.6±666.9
4	0.003±0.001	244.7±4.9	0.302±0.007	2.3 ± 0.7	0.0110 ± 0.0005	61.6 ± 2.2
5	0.001±0.001	452.5±16.7	0.077±0.003	7.9 ± 0.3	0.0079 ± 0.0030	88.2 ± 3.4
6	0.002±0.001	3465.7±48.8	0.070±0.002	10.4 ± 0.2	0.0053 ± 0.0005	125.1± 10.9

* Reported in our previous work.[15]

Table 2. Binding percentage of **1-6** to plasmatic proteins as measured in human plasma (HP) and human plasma containing site I (salicylic acid, SA) and site II (diazepam, DZP) markers.

	Bound fraction (%)		
	HP	**HP + SAL**	**HP + DZP**
AZT	13.8 ± 1.4	2.8±1.5	nd
1	33.2 ± 6.8	8.1 ± 2.6	nd
2	26.8 ± 0.5	1.8 ± 1.3	nd
3	34.1 ± 1.5	4.8 ± 1.5	nd
4	52.1 ± 5.3	51.2 ± 3.2	37.8 ± 1.4
5	59.7 ± 4.3	61.5 ±2.5	50.6 ± 5.9
6	72.5 ± 4.3	72.8 ± 3.2	48.8 ± 4.6

HP: human plasma. SA: salicylic acid. DZP: diazepam.

Table 3. Per-residue MMGBSA binding free energy decomposition analysis (Kcal/mol) of compounds **1**-**3** and SAL in Site I.

Contact	**AZT**	**1**	**2**	**3**	**SAL**
Tyr150	-1.35	-1.81	-1.10	-0.87	-
Ser192	-0.14	-0.22	-0.50	-0.65	-
Lys195	-1.17	-0.86	2.45	0.85	-
Gln196	0.51	-1.23	-1.04	-1.79	-
Lys199	-0.13	-0.85	-0.60	-0.87	-
Leu219	-	-	-	-	-0.40
Phe223	-	-	-	-	-0.21
Leu238	-	-	-	-	-1.27
Val241	-0.50	-0.70	-0.69	-0.76	-1.07
Cys245	-0.61	-0.07	-0.32	-0.51	-
Arg257	1.15	-8.62	-13.23	-14.04	-13.45
Leu260	-	-	-	-	-1.78
Ile264	-	-	-	-	-0.22
Ser287	-0.14	-0.41	-0.51	-0.20	-2.18
His288	-0.10	-5.33	-1.49	-0.12	-
Ile290	-	-	-	-	-1.81
Ala291	-0.24	-0.65	-1.16	-1.32	-1.76
ΔG_{sum} [a]	-2.72	-20.75	-18.10	-20.28	-24.15

Table 4. Per-residue MMGBSA binding free energy decomposition analysis (Kcal/mol) of compounds **4**-**6** and DZP in Site II.

Contact	DZP	4	5	6
Ser342	-	-1.14	-1.10	-
Glu382	-	-0.18	-0.12	-0.72
Glu383	-0.35	-1.80	-1.16	-4.11
Pro384	-0.69	-0.51	-1.04	-0.82
Leu387	-2.16	-1.89	-1.11	-3.84
Ile388	-2.93	-2.10	-1.61	-2.46
Asn391	-0.87	0.96	0.68	-0.34
Phe403	-0.44	-0.53	-0.76	-0.25
Leu407	-0.60	-0.56	-1.06	-0.19
Tyr411	-0.10	-	-	-
Leu430	-0.68	-0.64	-1.73	-1.08
Gly434	-0.37	-0.46	-0.83	-0.54
Ala449	-0.81	-0.33	-0.14	-0.41
Glu450	-0.54	-1.60	-1.44	-0.40
Leu453	-1.12	-1.41	-1.79	-1.35
Arg485	-0.62	-	-	-
Pro486	-	-0.10	-0.10	-0.59
Phe488	-	-0.71	-0.72	-0.18
Ala490	-	-	-	-1.35
Leu491	-	-0.25	-0.10	-0.63
ΔG_{sum}[a]	-12.26	-13.22	-14.13	-19.26

Table 5. Per-residue MMGBSA binding free energy decomposition analysis (kcal/mol) of compounds **4**-**6** in Site I.

Residues	4	5	6
Tyr150	-1.97	-3.60	-2.21
Ser192	-0.71	-1.17	-0.78
Lys195	1.97	1.26	0.93
Gln196	-0.74	0.61	-1.15
Lys199	3.29	1.16	3.53
Val241	-0.21	0.17	-0.28
Cys245	-0.39	-0.62	-0.85
Arg257	4.65	7.19	5.02
Ser287	-0.54	-0.54	-0.62
His288	-0.16	0.13	-0.66
Ala291	-1.32	-1.15	-0.43
ΔG_{sum}[a]	3.88	3.43	2.51

[a] Total sum of all the residue interactions.

Figure Captions

Figure 1. Molecular structures of: a) AZT, b) AZT prodrugs with oxalic acid (AZT-Ox) and aminoacids (AZT-Ox-AA), c) AZT prodrugs with dicarboxylic acids (**1-3**) and d) AZT double prodrugs (**4-6**) by derivatization of **1-3** with a methylated *l*-phenylalanine moiety.

Figure 2. a) Three-dimensional structure of HSA showing the different domains and subdomains. b) Stereoview of Site I including warfarin as ligand, and c) Stereoview of Site II including diazepam as ligand.

Figure 3. Concentration vs time profile of prodrugs **4**, **5**, and **6** in human plasma.

Figure 4. Interaction pattern of compounds **1** (a), **2** (b), **3** (c) and SAL (d) in site I of HSA.

Figure 5. Interaction pattern of DZP (a), **4** (b), **5** (c) and 6 (d) in site II of HSA.

Scheme 1. Activation (triphosphorylation) and inactivation (glucuronidation) pathways described for AZT

Scheme 2. Synthetic procedure for the obtention of prodrugs **4**-**6**.

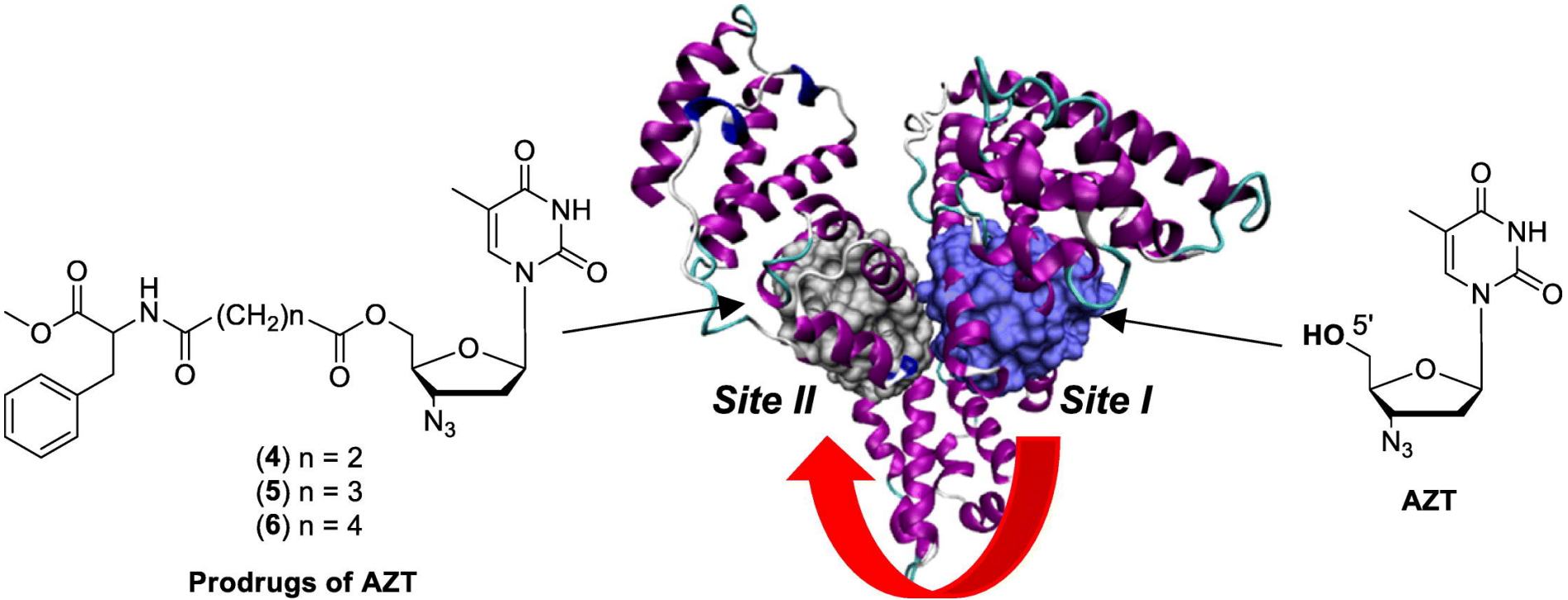

Graphics Abstract

a)

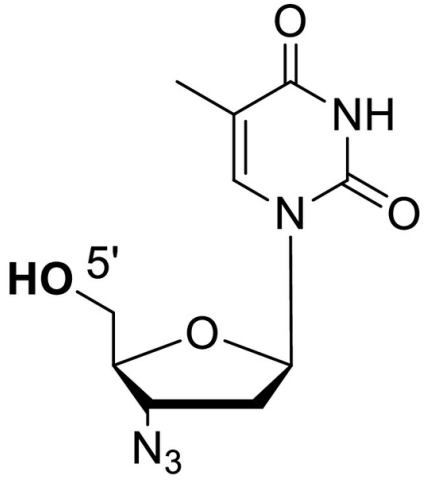

b)

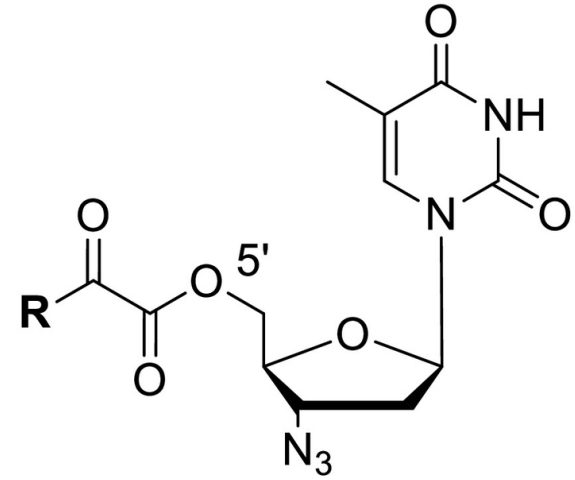

R = OH (**AZT-Ox**)
R = NH-aminoacid (**AZT-Ox-AA**)

c)

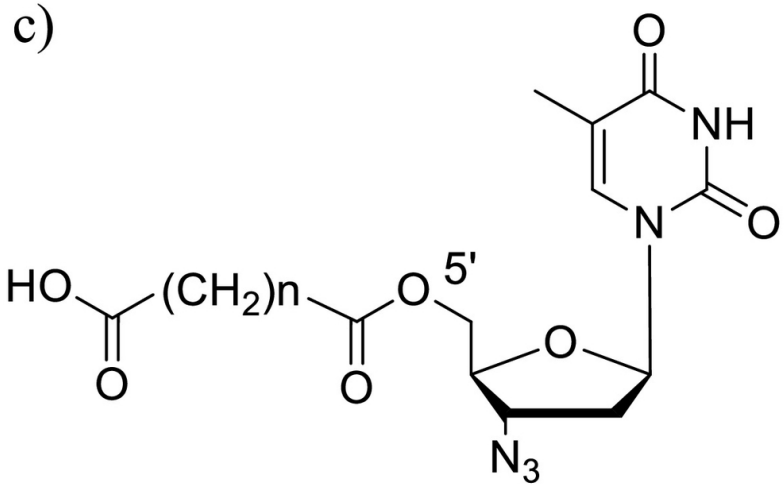

(**1**) n = 2
(**2**) n = 3
(**3**) n = 4

d)

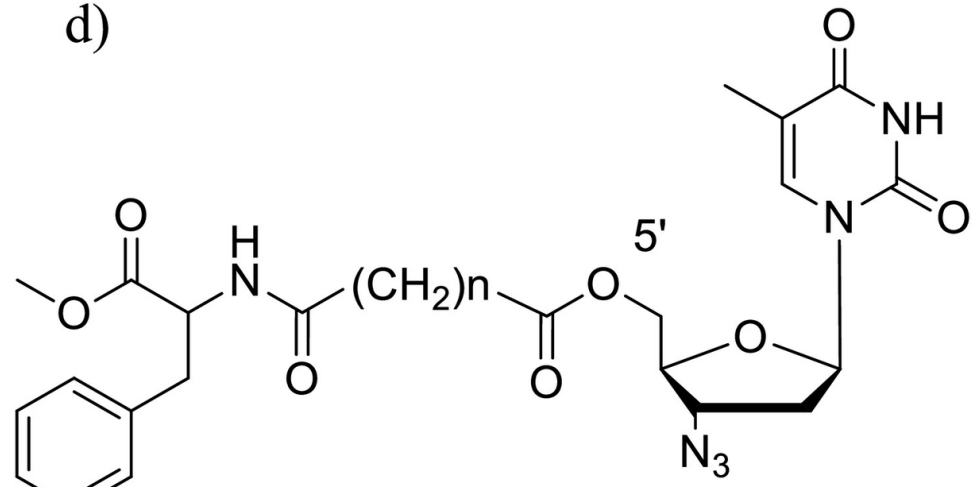

(**4**) n = 2
(**5**) n = 3
(**6**) n = 4

Figure 1

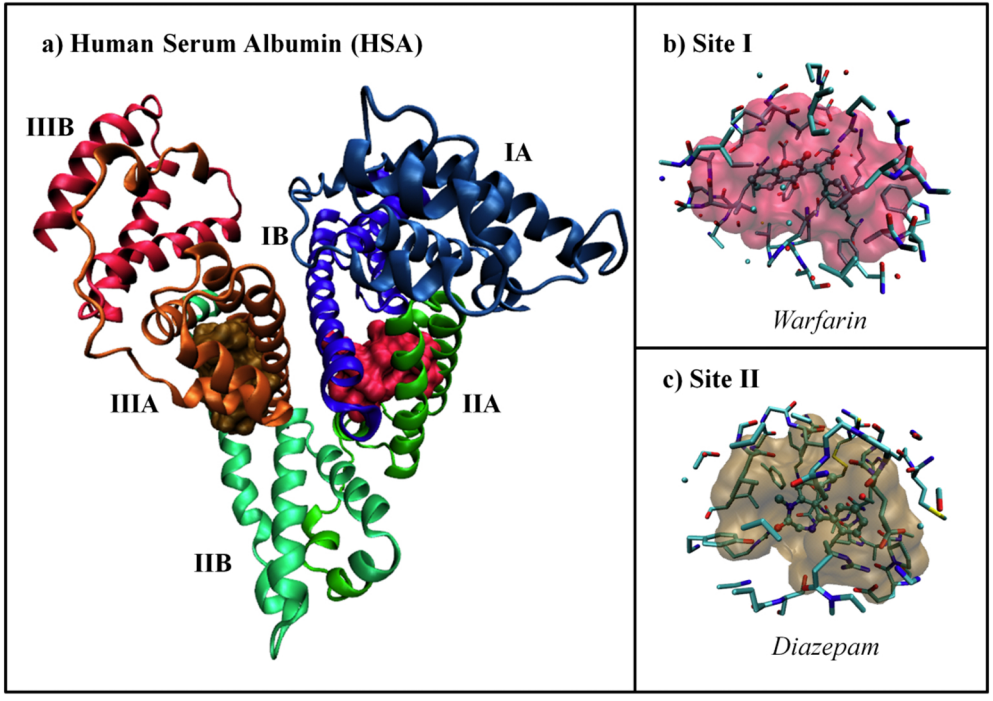
a) Human Serum Albumin (HSA)
IIIB
IA
IB
IIIA
IIA
IIB
b) Site I
Warfarin
c) Site II
Diazepam

Figure 2

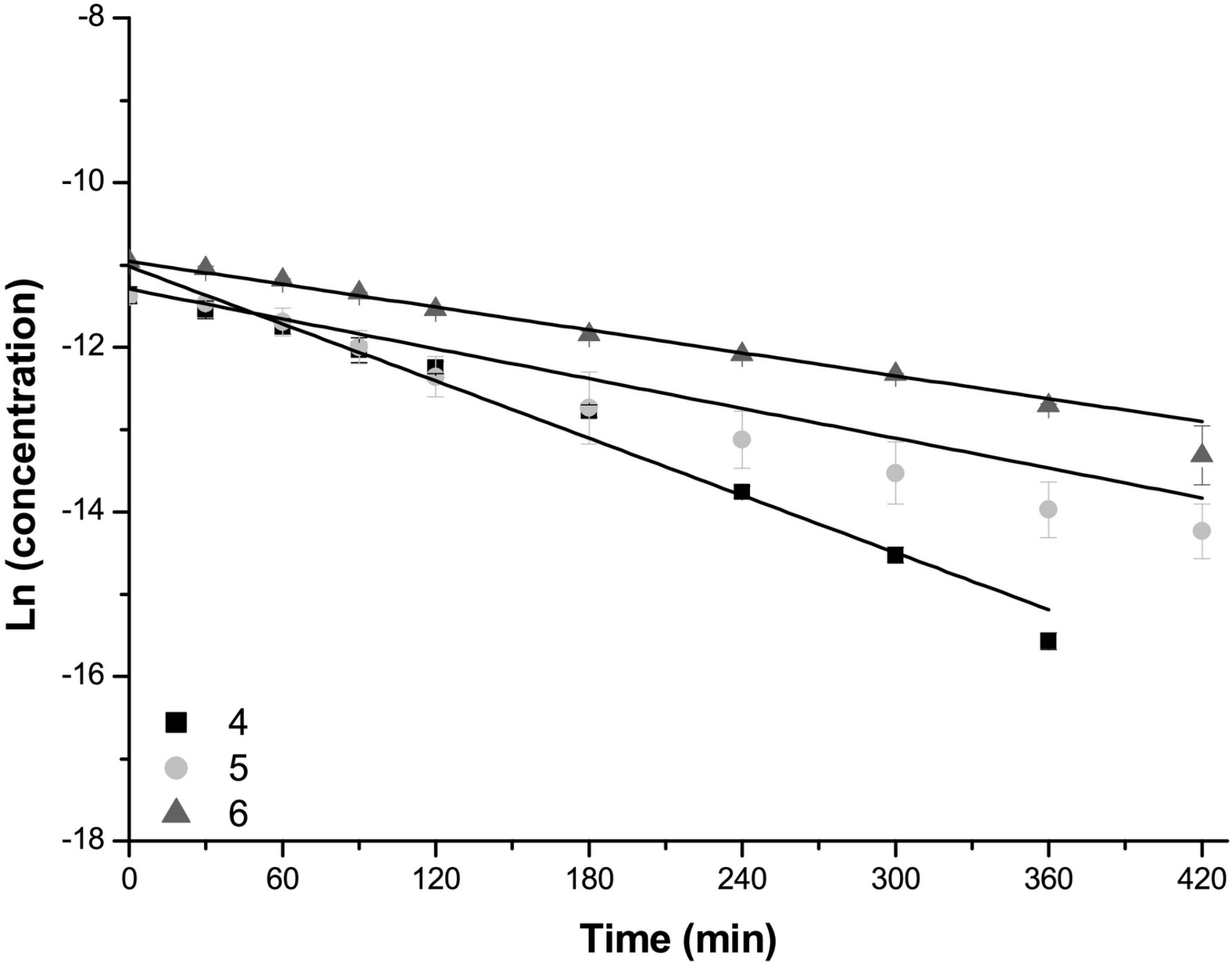
-8
-10
-12
-14
-16
-18
Ln (concentration)
0
60
120
180
240
300
360
420
Time (min)
4
5
6

Figure 3

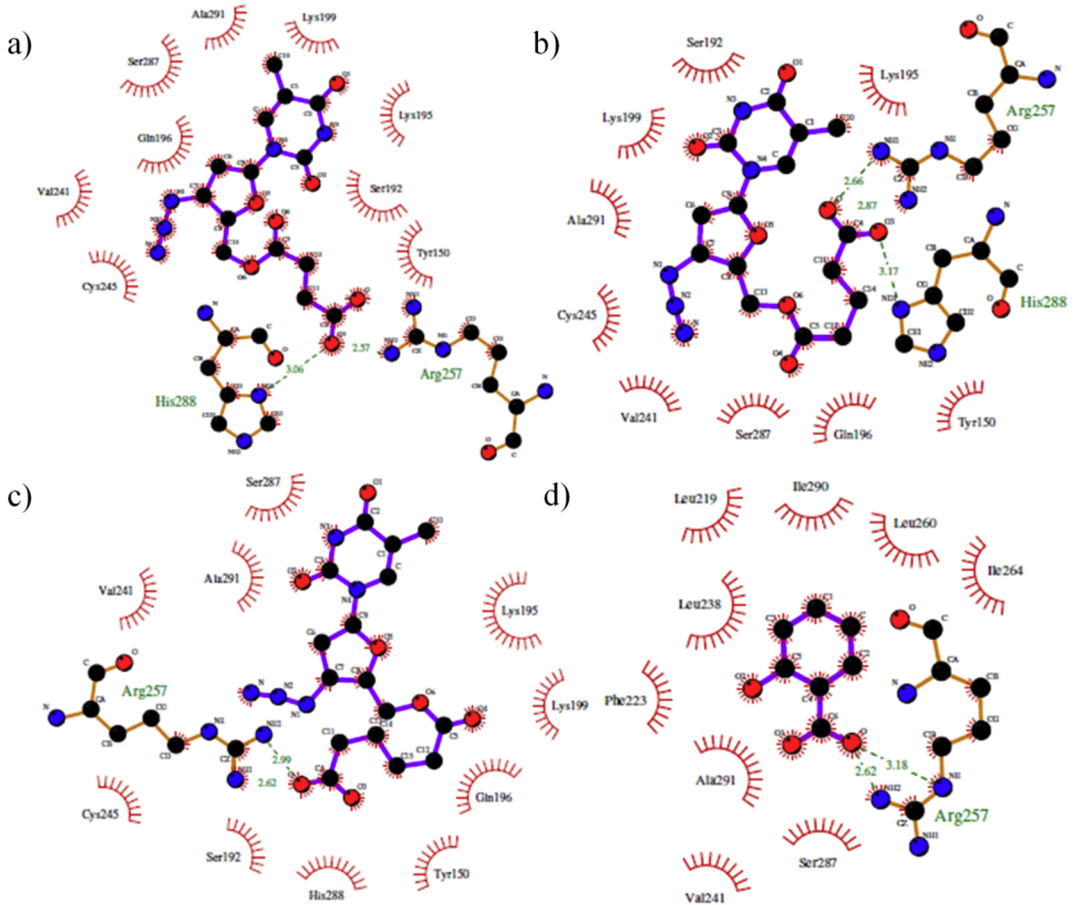
a)
Ala291
Lys199
Ser287
Lys195
Gln196
Val241
Ser192
Tyr150
Cys245
2.57
3.06
His288
Arg257
b)
Ser192
Lys195
Lys199
Arg257
2.66
2.87
Ala291
3.17
Cys245
His288
Val241
Ser287
Gln196
Tyr150
c)
Ser287
Val241
Ala291
Lys195
Arg257
2.99
2.62
Lys199
Cys245
Gln196
Ser192
Tyr150
His288
d)
Leu219
Ile290
Leu260
Ile264
Leu238
Phe223
Lys199
Ala291
2.62
3.18
Arg257
Ser287
Val241

Figure 4

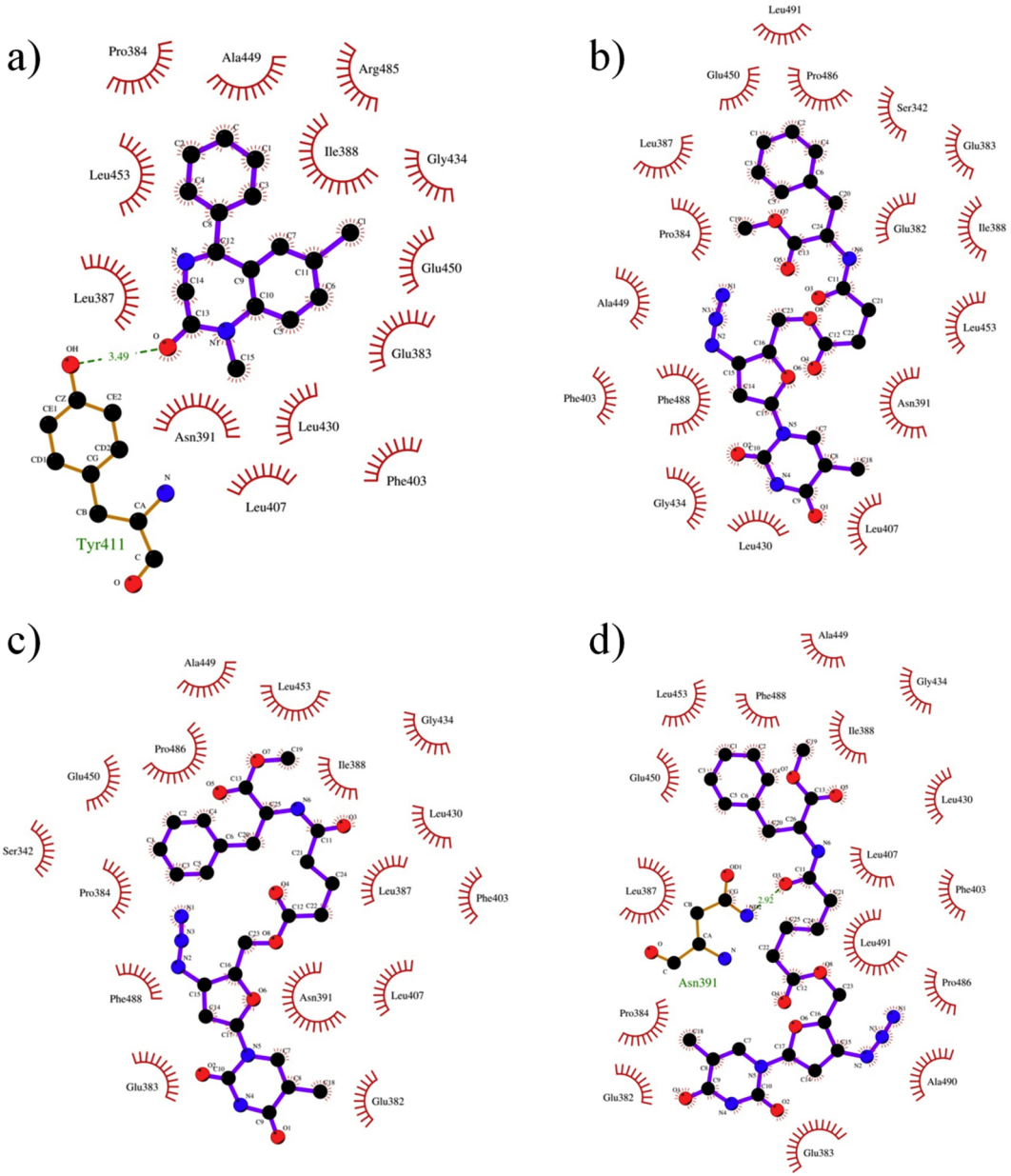
a)
Pro384
Ala449
Arg485
Ile388
Gly434
Leu453
Glu450
Leu387
Glu383
3.49
Asn391
Leu430
Phe403
Leu407
Tyr411
b)
Leu491
Glu450
Pro486
Ser342
Leu387
Glu383
Pro384
Glu382
Ile388
Ala449
Leu453
Phe403
Phe488
Asn391
Gly434
Leu407
Leu430
c)
Ala449
Leu453
Gly434
Pro486
Glu450
Ile388
Leu430
Ser342
Pro384
Leu387
Phe403
Phe488
Asn391
Leu407
Glu383
Glu382
d)
Ala449
Leu453
Phe488
Gly434
Ile388
Glu450
Leu430
Leu407
Leu387
Phe403
2.92
Leu491
Asn391
Pro486
Pro384
Ala490
Glu382
Glu383

Figure 5